Model for the unidirectional motion of a dynein molecule

Sutapa Mukherji
Department of Physics, Indian Institute of Technology, Kanpur 208016, India
(Received 13 October 2007; revised manuscript received 25 February 2008; published 19 May 2008)

Cytoplasmic dyneins transport cellular organelles by moving on a microtubule filament. It has been found recently that depending on the applied force and the concentration of the adenosine triphosphate molecules, dynein's step size varies. Based on these studies, we propose a simple model for dynein's unidirectional motion taking into account the variations in its step size. We study how the average velocity and the relative dispersion in the displacement vary with the applied load. The model is amenable to further extensions by inclusion of details associated with the structure and the processivity of the molecule.

DOI: 10.1103/PhysRevE.77.051916 PACS number(s): 87.16.Nn, 87.16.A−, 05.60.−k

I. INTRODUCTION

Dynein is a motor protein that moves on a microtubule filament to participate in certain activities inside a cell such as transport of vesicles, cell division, etc. [1]. Dynein moves toward the negative end of the microtubule and this feature is used by the cell, e.g., for the transport or aggregation of cellular organelles toward the nucleus of the cell. Based on their activities, dynein molecules are classified into two groups, namely, axonemal dynein and cytoplasmic dynein. Of these two, the axonemal dyneins work together in groups to produce rhythmic motions of cilia and flagella. The cytoplasmic dyneins, in which we are interested, perform, either in a group or alone, the job of transport of cargoes such as cytoplasmic vesicles, chromosomes, etc., along the microtubule filaments. Besides these dyneins, there are other kinds of motor proteins such as kinesin and myosin which are microtubule positive end directed and actin filament based, respectively. These motor molecules also perform similar jobs as dynein. However, in comparison with these motors, dynein molecules are exceptionally large and complex. Roughly, the dynein molecule consists of two to three heavy chain units each of which has a globular head domain (approximately 15 nm diameter) with special sites capable of adenosine triphosphate hydrolysis, and two elongated structures known as stalk and tail. The stalk and the tail bind the microtubule and the cargo, respectively. Because of the size, and also the difficulties in expressing and purifying the mutants, the progress in understanding the mechanism of dynein's motion [2–4] is slow.

In general, the movement of a motor molecule takes place in the following way. The adenosine triphosphate (ATP) molecule, which diffuses in the solution inside the cell, can get attached to specific regions or active sites in a motor's head. The motor molecule is capable of catalyzing a decomposition (hydrolysis) of this ATP into adenosine diphosphate (ADP), inorganic phosphate (P_i), and a significant amount of energy. This energy, so released, causes a conformational change in the molecule resulting in a motion relative to the microtubule. This process of hydrolysis repeats if the ATP concentration is sufficiently high and the motor molecule moves forward. In the case of dynein, the head domain consists of several sites at which ATP binding and unbinding or hydrolysis may take place. Although the details of the functional roles of these sites are still under investigation, it is believed that these sites are capable of controlling and regulating the motion of the dynein molecule.

Since the activities of motor proteins are force driven, it is important to know the response of the motion of the motor molecule to an externally applied force. The force generated by a motor molecule can be measured in single molecule experiments. For example, in optical trap experiments, a motor molecule is attached to a polystyrene bead which acts as a probe to monitor the movement of the motor molecule. The force on the bead due to the motor molecule is counteracted by a controlled backward force from the optical trap. The bead stays immobile if the backward force is strong enough to resist the force generated by the motor. The minimum force needed to hold the bead immobile is the stall force which is a measure of the force generated by the molecule.

An applied force, F, can affect the velocity in the following way. In general, a motor molecule moves due to the internal conformational changes and these conformational changes occur due to events such as ATP attachment or detachment and ATP hydrolysis. The process of ATP attachment is also dependent on the concentration of the ATP molecules inside the cell. These events take place with certain probabilities which determine their average rates. The external force may give rise to internal deformations because of which the ATP attachment or detachment rate and the hydrolysis rate change, thereby changing the average velocity, v, of the molecule. Thus, studying the force-velocity relationship both theoretically and experimentally is crucial for predicting how exactly various processes are affected by the force. In addition to this systematic force, there can be thermal noise which also affects the velocity of dynein by changing different rate constants. In the case of such a stochastic displacement of the molecule, it is possible to define an effective diffusion constant $D_{\text{eff}}=[\langle x^2(t)\rangle-\langle x(t)\rangle^2]/(2t)$ which is a measure of the fluctuation in the displacement. Here, $\langle\cdots\rangle$ denotes the statistical average. In terms of this diffusion constant, one can also define a natural time scale a^2/D_{eff} which is the time required for the molecule to diffuse a natural length scale, a. The distance traveled during this time due to the drift velocity v is $v\times a^2/D_{\text{eff}}$. The ratio of these two distances is often referred to as the randomness parameter [5,6]

$$r = 2D_{\text{eff}}/av. \quad (1)$$

This parameter derived earlier for kinesin has been found useful for understanding the internal mechanism of the molecule.

From the structural studies of dynein, it is believed that the dynein based transport in the cell is quite different and robust in comparison with other motors. However, experimentally, the mechanism of dynein's function is not yet fully understood. For example, a recent experiment [4] that demonstrates 8 nm step size for a cytoplasmic dynein contradicts an earlier observation [3] that the step size of dynein increases from 8 nm to 16, 24, and 32 nm as the strength of the applied force reduces. Various step lengths found in [3] are multiples of a unit step size $a=8$ nm, which corresponds to a certain periodicity of the microtubule filament. In addition, the results of [4] on the average velocity of dynein and the value of the stall force are significantly different from those of Ref. [3]. A single molecule experiment on axonemal dynein has also demonstrated stepwise displacements of 8 nm size [7]. In view of these differences, a theoretical model that can take into account the wide step size variation of the molecule and can predict how, in this case, the velocity depends on the applied force appears meaningful. In addition, this analysis, which is going to be based on several assumptions on how various sites in a dynein's head participate in regulating the motion, is expected to help explain the mysterious roles of these sites. Although some theoretical work has been done to understand various activities of dynein, such as rhythmic beating of axonemal dyneins [8], unidirectional motion of dyneins [9,10], and geared motion of dynein to explain its force-dependent step size [11], so far there has been no analytical approach to understand how the variable step size can affect the average velocity.

Based on the recent structural observation, we propose a model in which one can incorporate 8 nm and other longer jumps and study how this wide variation of the step size affects the average velocity. In case of variations in the step size, one needs to do a detailed fluctuation analysis to obtain the distributions of the step length and the number of steps in a given time. The definition of the randomness parameter in Eq. (1), therefore, needs to be modified appropriately, possibly, by the inclusion of an average step length. However, in terms of a as the smallest step, the randomness parameter helps us observe how the step size variation affects the fluctuation in the displacement of the molecule. Although, for simplicity, we include only a few essential structural and mechanochemical details [9], the model is flexible enough to incorporate other details.

The paper is organized as follows. In Sec. II, we discuss the basic assumptions based on which the model is built. The analysis of the model is presented in Sec. III. Section III is divided into two subsections as we consider different variants of the model by including longer jumps of the dynein molecule. We conclude the paper with a summary of the work in Sec. IV.

II. BASIC ASSUMPTIONS OF THE MODEL

It is known that the dyenin's head domain consists of six subdomains of the AAA family of proteins arranged in the form of a ring around a central cavity [12]. Out of these AAA subdomains, only four are capable of ATP binding with varying binding affinities [13,14]. ATPase activities of these different AAA subdomains are subjects of experimental investigations. Although AAA1 is believed to be the primary site of ATP hydrolysis which powers the motion of the molecule, recent experimental observations support hydrolytic activities of other AAA subdomains [14–16]. Some of the studies elucidating the functional roles of the AAA subdomains indicate that other AAA subdomains may play various regulatory roles by altering the hydrolysis of the primary site and subsequently affecting the molecular function, or by modulating the efficiency of the coupling between the microtubule binding site and the primary site [13,14,17]. In our analysis, we call the subdomains AAA2–AAA4 secondary sites.

In view of the inherent complexity of dynein and our evolving understanding of how various components of the molecule function, it appears worthwhile to propose a model with the following assumptions.

(1) For our entire analysis, we assume the dynein molecule to be effectively single headed [9]. Studies on head-head coordination [18] during the processive movement of dynein suggest that similar to kinesin and myosin, the rear head of dynein may sense a pulling force from the forward head and this force may modulate the kinetic steps appropriately to coordinate the forward motion. The hydrolysis presumably takes place alternatively in each head and at a given step a single head proceeds forward in a hand-over-hand fashion. Since these details of the head coordination are not an issue here, both the heads can be thought of as a composite object—a single head. The effect of the pulling force in the ATPase activities of the head is assumed to be incorporated through the rates. The two-head problem can be studied if additional information is known about how the force exactly modulates the kinetic steps in the head.

(2) We assume that there are only two ATP binding sites (subdomains) of which one is a primary site (P) and the other one is a secondary site (S). This is modified later by including more numbers of secondary sites.

(3) In our analysis, only the primary site is capable of ATP hydrolysis. It is possible to incorporate hydrolytic activities of other secondary sites considering that such additional hydrolysis may change the driving force or the regulatory mechanism of dynein. We plan to consider these processes in our future analysis elsewhere.

(4) Rates of binding or unbinding of ATP to or from the primary site are denoted by $k_{\text{on},1}$, $k_{\text{off},1}$, respectively. Subscripts 2 and 3 with these rates imply binding or unbinding processes at the secondary sites. It is assumed that the primary site has the highest affinity to the ATP molecule. Therefore, if the primary site is empty, it first gets filled even in the presence of an empty secondary site. Similarly, ATP unbinding from the primary site does not take place if there are occupied secondary sites. These rules hold throughout the entire analysis.

(5) To start with, it is assumed that ATP hydrolysis at the primary site causes the dynein to jump the smallest distance $a=8$ nm. This can be modified further. The distance a dynein molecule can jump after a hydrolysis can change de-

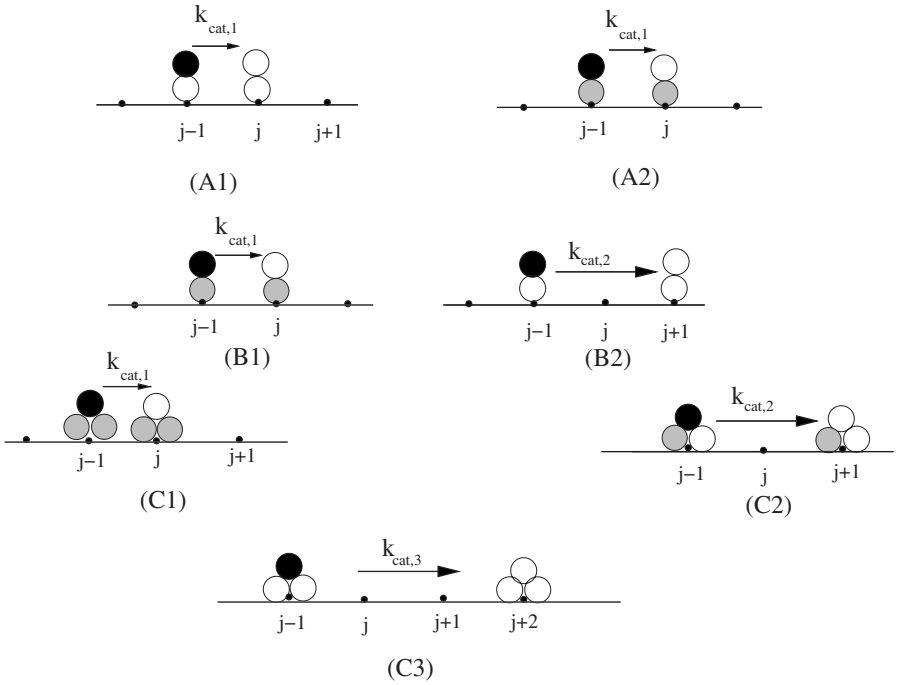

FIG. 1. Various moves of the dynein molecule, considered in the text, are shown here. AAA subdomains or ATPase activity sites are represented by circles. The filled, shaded, and unfilled circles represent ATP occupied primary site, ATP occupied secondary site, and empty primary or secondary site, respectively. Various moves take place after hydrolysis in the primary site with the rates as indicated in Eq. (2). (A1), (A2) A jump by a distance a always. The dynein molecule is assumed to have two active AAA subdomains. (B1), (B2) The molecule jumps a distance a (or $2a$) when the secondary site is in an ATP-bound (or ATP-unbound) state. The dynein molecule has two active AAA subdomains. This case has been discussed in Sec. III A 2. (C1)–(C3) Three possible moves of lengths a, $2a$, and $3a$ depending on the number of ATP-bound secondary sites. The dynein molecule has three active AAA subdomains. This case has been discussed in Sec. III B.

pending on whether the secondary site is occupied or unoccupied. If the secondary site is occupied, the dynein molecule jumps a distance a after a hydrolysis. In case the secondary site is unoccupied, the dynein molecule moves $2a$ distance ahead at a time after a hydrolysis. In the presence of two secondary sites, the dynein can jump $3a$ distance at a time after one hydrolysis if both secondary sites are empty. Jumps of length $2a$ or a are possible if one or both of the secondary sites are occupied, respectively. The hydrolysis processes, which trigger jumps of length a, $2a$ or $3a$, take place at rates $k_{\text{cat},1}$, $k_{\text{cat},2}$, and $k_{\text{cat},3}$, respectively. A schematic diagram, indicating various moves described here, is presented in Fig. 1.

(6) Our analysis is based on the assumption that the time required for a transition is much smaller than the time between two successive transitions. In addition, we also assume that the thermal relaxation of the molecule after a transition is much faster compared to the transition rate [19,20]. This allows us to assume quasiequilibrium for transitions from one state to the other over various free energy barriers. At temperature T, the rate constants are, therefore, expected to depend exponentially on $[FD/(k_BT)]$, where D is an appropriate parameter in the units of length and k_B is the Boltzmann constant. Our next assumption is related to the explicit dependences of various rate constants on the load.

(7) It is expected that the mechanochemical cycle is affected by the applied load, in particular, since we know that the motion of the motor comes to a halt when the applied opposing force is sufficiently high. One way of implementing this load dependence is by considering a load-dependent hydrolysis rate as

$$k_{\text{cat},i} = A(s)k_{\text{cat},0} \exp[-\alpha Fd(s)/k_BT], \tag{2}$$

where $i=1,2,3$ and $d(s)=i\times a$ is the distance the molecule jumps after the hydrolysis. $k_{\text{cat},0}$ is the hydrolysis rate for no load. α is the load distribution factor for hydrolysis. In general, there is no restriction on the sign of α. Here, it is more intuitive to assume α to be positive since the hydrolysis rate should decrease with the increase in the opposing external force. There exists, however, one restriction on α that the sum of the load distribution factors for hydrolysis and reverse hydrolysis should be unity. The possibilities of reverse hydrolysis are not taken into account in order to appreciate the crucial features of the results when the number of parameters is less. ATP hydrolysis is assumed to be enhanced if at least one secondary site binds ATP. This is taken care of by $A(s)$ which is 1 if the secondary site is ATP-bound and is equal to 0.01 otherwise. In the case of jumps by only a distance a, we have only one hydrolysis rate $k_{\text{cat},1}$, irrespective of whether the secondary site is occupied or unoccupied by an ATP molecule. In this case, $A(s)=1$ always. In the case of jumps by distance a or $2a$, we choose the values of $A(s)$ as prescribed here.

As has been proposed earlier [9], we also assume that the ATP binding affinities of the secondary sites are dependent on the load as

$$k_{\text{on},2-4} = k_{\text{on},2-4}(F=0)\exp(Fd_0/k_BT), \tag{3}$$

where d_0 is an adjustable parameter in the units of length. For obtaining all the results, we choose the value of d_0, to be the same as that in Ref. [9].

III. ANALYSIS OF THE MODEL

The forward motion can be described through equations that describe time evolutions of certain variables on a one-dimensional lattice. A variable, here, represents the probability of a molecule being at a given lattice site at a time t with a given configuration of its ATPase activity sites. For example, a variable $S_j^{\alpha\beta}$ represents the probability of a molecule with two AAA sites being at the jth lattice site with primary and secondary sites being in α and β states, respectively. α and β can have values 0 or 1 if a site is unoccupied or occupied by an ATP molecule. The time evolution equations for all the variables, say, $S_j^{00}, S_j^{01}, S_j^{10}, S_j^{11}$ for a molecule with two ATPase sites, can be combined into a matrix equation. This matrix equation, thus, represents the time evolution of the column matrix ρ_j whose elements are the probability variables mentioned above. This equation can further be recast as a matrix equation describing the time evolution of the column matrix $\Sigma_{j=-\infty}^{j=\infty}\zeta^j\rho_j$. ζ is an arbitrary parameter and as we shall discuss below, the determination of the average velocity requires ζ to be unity.

In the following subsection, we discuss the specific case where the molecule jumps by a distance a only irrespective of the ATP occupancy state of the secondary site. The derivation of the velocity is presented here in detail. This method allows us to look at the variation of the randomness parameter with the applied opposing force. The same method is generalized in the next subsections for the cases where the molecule can make longer jumps depending on the ATP occupancy state of the secondary sites.

A. Dynein with one primary and one secondary site

1. Jumps by a distance a

The time evolution of the four probability variables corresponding to all four configurations of the ATP binding sites of a dynein at the jth site is governed by the equations

$$\frac{dS_j^{00}}{dt} = k_{\text{off},1}S_j^{10} + k_{\text{off},2}S_j^{01} + k_{\text{cat},1}S_{j-1}^{10} - k_{\text{on},1}S_j^{00}, \tag{4}$$

$$\frac{dS_j^{01}}{dt} = k_{\text{cat},1}S_{j-1}^{11} - k_{\text{on},1}S_j^{01} - k_{\text{off},2}S_j^{01}, \tag{5}$$

$$\frac{dS_j^{10}}{dt} = k_{\text{off},2}S_j^{11} + k_{\text{on},1}S_j^{00} - k_{\text{off},1}S_j^{10} - k_{\text{on},2}S_j^{10} - k_{\text{cat},1}S_j^{10}, \tag{6}$$

$$\frac{dS_j^{11}}{dt} = k_{\text{on},1}S_j^{01} + k_{\text{on},2}S_j^{10} - k_{\text{cat},1}S_j^{11} - k_{\text{off},2}S_j^{11}. \tag{7}$$

These equations can be written in a matrix form as

$$\frac{d[\rho_{\mathbf{j}}]}{dt} = [\mathbf{A}][\rho_{\mathbf{j}}] + [\mathbf{B}][\rho_{\mathbf{j-1}}], \tag{8}$$

where

$$\rho_{\mathbf{j}} = \begin{pmatrix} S_j^{00} \\ S_j^{01} \\ S_j^{10} \\ S_j^{11} \end{pmatrix}, \tag{9}$$

and $\mathbf{A}$ and $\mathbf{B}$ are matrices whose elements are the various rate constants of the differential equations. Multiplying both sides of Eq. (8) with ζ^j and summing over all possible values of j, we have

$$\frac{d}{dt}\sum_{j=-\infty}^{\infty}\zeta^j\rho_j = [\mathbf{A}]\sum_{j=-\infty}^{\infty}\zeta^j\rho_j + [\mathbf{B}]\sum_{j=-\infty}^{\infty}\zeta^j\rho_{j-1}. \tag{10}$$

In terms of $G(\zeta,t)=\Sigma_{j=-\infty}^{\infty}\zeta^j\rho_j$, the above equation is

$$\frac{d}{dt}G(\zeta,t) = ([\mathbf{A}] + \zeta[\mathbf{B}])G(\zeta,t) = [\mathbf{R}(\zeta)]G(\zeta,t), \tag{11}$$

where

$$[\mathbf{R}(\zeta)] = \begin{pmatrix} -k_{\text{on},1} & k_{\text{off},2} & k_{\text{off},1}+\zeta k_{\text{cat},1} & 0 \\ 0 & -(k_{\text{on},1}+k_{\text{off},2}) & 0 & \zeta k_{\text{cat},1} \\ k_{\text{on},1} & 0 & -(k_{\text{off},1}+k_{\text{on},2}+k_{\text{cat},1}) & k_{\text{off},2} \\ 0 & k_{\text{on},1} & k_{\text{on},2} & -(k_{\text{cat},1}+k_{\text{off},2}) \end{pmatrix} \tag{12}$$

$[\mathbf{R}(\zeta=1)]$ is a transition matrix with the sum of all elements in a column being zero. The largest eigenvalue of the matrix $\mathbf{R}(\zeta=1)$ is, therefore, zero.

Our final aim is to find out the average velocity $\langle j\rangle/t$ and the diffusion constant of the dynein molecule. It has been shown earlier that the average velocity and the effective diffusion constant in such a case can be found from the relations [21,22]

TABLE I. Model parameters.

Symbol	Value	Meaning
k_BT	4.1 pN nm	Thermal energy
$k_{off,1}$	10 s^{-1}	Rate of unbinding of an ATP molecule from the primary site
$k_{off,2}$	250 s^{-1}	Rate of unbinding of the first ATP molecule from one of the secondary sites
$k_{off,3}$	250 s^{-1}	Rate of unbinding of the second ATP molecule from one of the secondary sites
$k_{on,1}$	4×10^5 M^{-1} s^{-1} [ATP]	Rate of ATP binding to the primary site
$k_{on,2}(F=0)$	4×10^5 M^{-1} s^{-1} [ATP]	Rate of first ATP binding at the secondary sites under zero load
$k_{on,3}(F=0)$	$k_{on,2}(F=0)/4$	Rate of second ATP binding at the secondary sites under zero load
d_0	6 nm	An adjustable length as introduced in Eq. (3)
$k_{cat,0}$	55 s^{-1}	Hydrolysis rate under zero load
α	0.3	Load distribution factor

$$\langle v\rangle = a\frac{\langle j\rangle}{t} = a\lambda_l'(1), \quad D_{\text{eff}} = \frac{a^2}{2}[\lambda_l''(1)+\lambda_l'(1)], \tag{13}$$

where $\lambda_l(\zeta)$ is the largest eigenvalue of $[\mathbf{R}(\zeta)]$ and the primes denote derivatives of λ with respect to ζ.

In order to find out the largest eigenvalue, it is necessary to solve the characteristic equation,

$$\text{Det}[\mathbf{R}(\zeta)-\lambda\mathbf{I}] = 0. \tag{14}$$

The characteristic equation can be solved for the eigenvalues straight away. However, in order to find the derivative of the largest eigenvalue at $\zeta=1$, it is convenient to substitute $\zeta=1+\delta$, and $\lambda=\delta\lambda'(1)+\frac{\delta^2}{2}\lambda''(1)$ in Eq. (14), and then find out $\lambda_l'(1)$ and $\lambda_l''(1)$ by equating coefficients of δ and δ^2, respectively, to zero. The average velocity found this way is

$$v = a\frac{k_{cat,1}k_{on,1}[k_{cat,1}k_{off,2}+k_{off,2}k_2+k_{on,1}k_2]}{(k_{cat,1})^2k_{off,2}+k_{cat,1}(k+k_{off,2}k_2+2k_{off,2}k_{on,1})+(k_{off,2}+k_{on,1})(k_{off,1}k_{off,2}+k_{on,1}k_2)}, \tag{15}$$

where, $k=k_{off,1}k_{off,2}+k_{on,1}k_{on,2}$ and $k_2=k_{off,2}+k_{on,2}$. The expression for the diffusion coefficient can be obtained in a similar way. Since the diffusion coefficient involves a more complicated algebraic dependence on various rates, we avoid mentioning the expression here. Instead, we focus on the variation of the randomness parameter with the applied force later.

Using the values of various model parameters as listed in Table I, we plot the force-velocity curve for two different ATP concentrations in Fig. 2. Since the hydrolysis rate decreases with the force, the velocity is ultimately expected to decrease with the force when force is large. It can be seen from Eq. (15) that the velocity decreases exponentially as $v\sim k_{cat,1}=A(s)k_{cat,0}\exp[-\alpha Fd(s)/k_BT]$ for large force. For moderate force, there is a possibility of an increase in the velocity. This is due to $k_{on,2}$ which increases with the force as per Eq. (3) and enhances the probability of the molecule being in the state S_j^{11}. The velocity increases as a result of hydrolysis in this state. This can be also verified by choosing $k_{on,2}$ to be independent of the force in which case the velocity curve decreases monotonically for all values of the force. For higher values of ATP concentration, the increase in the velocity becomes less pronounced and it eventually disappears for high ATP concentration. The increase in the velocity at low ATP concentration is not present in the experimental observations of [4]. However, it may not be appropriate to compare these results with the experiments of [4] mainly because of the simplistic approach of the model where dy-

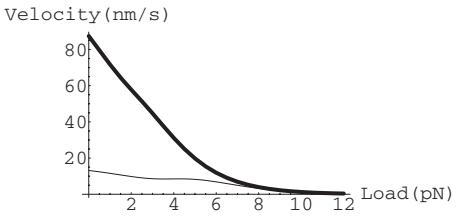

FIG. 2. A plot of the velocity (nm s^{-1}) with force (pN) for different ATP concentrations. The molecule can move forward by jumping a distance a only. The thin and thick lines correspond to [ATP]=5 μM, 40 μM, respectively.

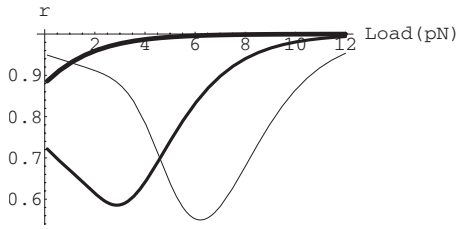

FIG. 3. A plot of the randomness parameter, r, with the applied force (pN) at various ATP concentrations. In this case the molecule can move forward by a distance a only. Three solid lines with increasing thickness correspond to ATP concentrations, [ATP] $=5\ \mu$M, 40 μM, 2 mM, respectively.

nein has been assumed to be single-headed with less number of secondary sites and with a very simple kinetic cycle without any reversal of hydrolysis or other additional hydrolysis. As we shall show later, the velocity changes significantly in the low force regime, as the possibility of longer jumps is incorporated. The variation of the randomness parameter r with the force, for given concentrations of ATP molecules, appears as in Fig. 3.

At low ATP concentrations, the randomness parameter initially decreases with the force in the moderate force regime. As the force is increased further, the randomness parameter increases and approaches 1. The increase in the velocity around the same values of force seems to be a reason for the decrease in r for low concentrations of ATP.

2. Possibility of jumps by a distance 2a

In the following, we incorporate the possibility of jumps by a distance $2a$. The dynein molecule moves forward by a distance a or $2a$ after a hydrolysis if the secondary site is in an ATP-bound or unbound state, respectively [see Figs. 1(B1) and 1(B2)]. Equation (2) shows that the hydrolysis rate, $k_{\mathrm{cat},1}$, which triggers a shorter jump, needs to be distinguished from the hydrolysis rate, $k_{\mathrm{cat},2}$, which powers a longer jump. Less binding affinity of the secondary site at a low force ensures that there can be larger jumps that are triggered by a hydrolysis whose rate increases as the value of the force decreases. Thus, we expect a significant change in the average velocity in the low force region from that of the case where the molecule jumps only by a distance a. The time evolution of the four probability variables are given as

$$\frac{dS_j^{00}}{dt} = k_{\mathrm{off},1}S_j^{10} + k_{\mathrm{off},2}S_j^{01} + k_{\mathrm{cat},2}S_{j-2}^{10} - k_{\mathrm{on},1}S_j^{00}, \tag{16}$$

$$\frac{dS_j^{01}}{dt} = k_{\mathrm{cat},1}S_{j-1}^{11} - k_{\mathrm{on},1}S_j^{01} - k_{\mathrm{off},2}S_j^{01}, \tag{17}$$

$$\frac{dS_j^{10}}{dt} = k_{\mathrm{off},2}S_j^{11} + k_{\mathrm{on},1}S_j^{00} - k_{\mathrm{off},1}S_j^{10} - k_{\mathrm{on},2}S_j^{10} - k_{\mathrm{cat},2}S_j^{10}, \tag{18}$$

$$\frac{dS_j^{11}}{dt} = k_{\mathrm{on},1}S_j^{01} + k_{\mathrm{on},2}S_j^{10} - k_{\mathrm{cat},1}S_j^{11} - k_{\mathrm{off},2}S_j^{11}. \tag{19}$$

Proceeding in a similar way as the one-step case, we may combine the differential equations in a single matrix equation

$$\frac{d}{dt}G(\zeta,t) = [\mathbf{R}(\zeta)]G(\zeta,t), \tag{20}$$

where

$$[\mathbf{R}(\zeta)] = \begin{pmatrix} -k_{\mathrm{on},1} & k_{\mathrm{off},2} & k_{\mathrm{off},1} + \zeta^2 k_{\mathrm{cat},2} & 0 \\ 0 & -(k_{\mathrm{on},1} + k_{\mathrm{off},2}) & 0 & \zeta k_{\mathrm{cat},1} \\ k_{\mathrm{on},1} & 0 & -(k_{\mathrm{off},1} + k_{\mathrm{on},2} + k_{\mathrm{cat},2}) & k_{\mathrm{off},2} \\ 0 & k_{\mathrm{on},1} & k_{\mathrm{on},2} & -(k_{\mathrm{cat},1} + k_{\mathrm{off},2}) \end{pmatrix} \tag{21}$$

and $G(\zeta,t)$ is the same as that defined earlier. The procedure for finding out the average velocity is the same as before. Figure 4 shows a comparison of velocities for a pure single step jump and for the case where both one- and two-step jumps are possible.

The figure shows that the average velocity in the two-step case reduces when the force is small. In the case of a jump by a distance a only, the forward move takes place at a much higher rate. Since in the two-step case, single steps are not allowed when the secondary site is empty and the allowed larger moves take place at a much lower rate, the average velocity reduces. The force-velocity plots for different ATP concentrations are shown in Fig. 5.

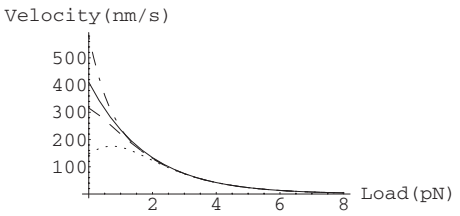

FIG. 4. A plot of the velocity with load at ATP concentration [ATP]=2 mM. The thin solid line and the dashed line correspond to the one-step and two-step cases, respectively. The dashed-dotted line represents the average velocity for the three-step jump. The dotted line represents the average velocity of the molecule with possibilities of a three-step jump with $k_{\mathrm{cat},2}$ reduced to $k_{\mathrm{cat},2}$ $=0.55\ \exp(-\frac{0.3\times 16\times F}{4.1})$.

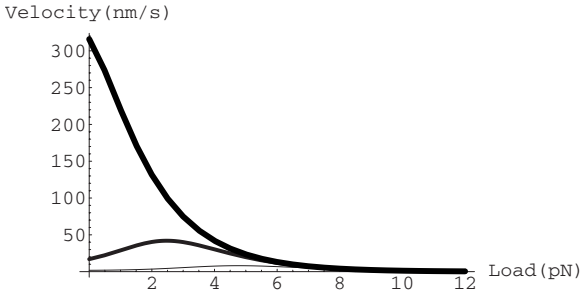

FIG. 5. Force-velocity plot for ATP concentrations 5 μM, 40 μM, and 2 mM. Lines with increasing thickness correspond to higher ATP concentrations. The molecule is allowed to jump by a distance $2a$ at a time if the secondary site is empty.

Introducing the possibility of two-step jumps increases the fluctuation in the displacement at low forces (see Fig. 6). This is likely to be the case since for low force, two-step jumps are more probable than for a high value of force. At high forces, the probability of longer steps decreases and the two plots merge.

B. Dynein with one primary and two secondary sites: Possibility of jumps by a distance $3a$

As further improvement toward the more realistic picture, we include two secondary sites. With three sites, there are now possibilities of jumps by a distance $3a$ in one move [see Fig. 1(C1)–(C3)]. This happens if no secondary site is occupied. With two secondary sites, the dynein molecule at the jth site can remain in eight possible states with probabilities $S_j^{000}, S_j^{001}, S_j^{010}, S_j^{100}, S_j^{011}, S_j^{101}, S_j^{110}, S_j^{111}$, evolution of which can be written in a way similar to that mentioned before.

The average velocity calculated for this case is shown in Fig. 4 along with the previous results for comparison. The average velocity is quite sensitive to the hydrolysis rates. It can be seen that lowering $k_{\text{cat},2}$ to $k_{\text{cat},2}=0.55 \times \exp(-\frac{0.3\times 16\times F}{4.1})$, causes a significant decrease in the average velocity. The concentration of ATP has significant effects on the average velocity. This is clear from the force-velocity plot in Fig. 7 for different ATP concentrations.

IV. SUMMARY

Dynein's structure is known to be fundamentally different from other motor proteins such as kinesin and myosin. It is believed that the complexity in the structure of dynein leads to a robust motion and leaves more opportunity of regulation of the motion at multiple levels. Due to its complexity, our knowledge about how dynein functions has been limited. One of the single molecule experiments suggests that unlike other motor proteins, dynein has a wide step size variation and the step length of dynein can be 8, 16, 24, or 32 nm depending on the strength of the opposing force. It has been predicted that the step size is around 32 nm for low or no load situations and the step size decreases as the strength of the force increases. One of the more recent experiments, however, demonstrates a fixed, load-independent step size close to 8 nm and different results regarding the value of the stall force and its dependence on the ATP concentration.

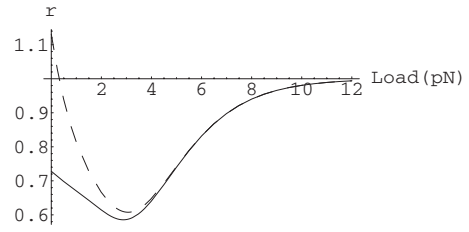

FIG. 6. A plot of the randomness parameter with load at [ATP]=40 μM. The solid and the dashed line correspond to the case where the molecule can jump a distance a or $2a$, respectively.

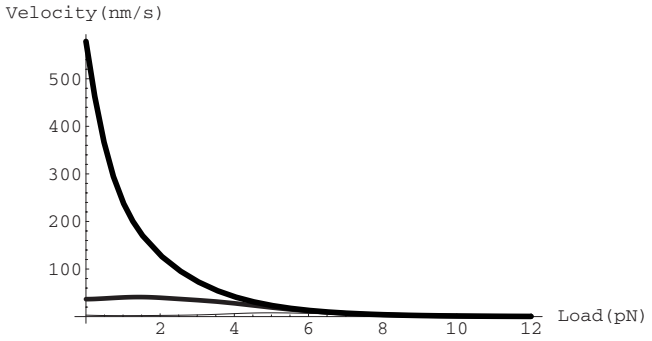

FIG. 7. A plot of velocity with load at different ATP concentrations. Three solid lines with increasing thickness correspond to [ATP]=5 μM, 40 μM, and 2 mM. The molecule is allowed to jump a distance $3a$ at a time if no secondary site is in the ATP bound state.

Since these experiments give different views about the step length and other properties of dynein, we propose our theoretical model to see the effect of step size variation on the average velocity of the molecule and the fluctuation in its displacement. Our model is based on certain simplifications. We assume that the head domain has a primary site which is primarily responsible for ATP hydrolysis that drives the motion and a maximum of two secondary sites which can regulate the motion through ATP binding. The force induced reduction of the step size is introduced through the assumption that the opposing force increases the binding affinity of the secondary site and the molecule makes a shorter jump if more numbers of secondary sites are in ATP bound states. Through this model, it is possible to understand analytically how the velocity changes as longer jumps are introduced in dynein's motion at a given ATP concentration. At low ATP, we find an initial increase in the velocity with the force before it finally decreases. This increase in the velocity is not seen at high ATP concentrations. It appears that this increase is partly due to the force-dependent binding affinity of the secondary sites. We also study the randomness parameter introduced in Eq. (1). This quantity gives an estimate of the variation of the fluctuation in the displacement with the applied opposing force. The possibility of larger jumps under low-load condition introduces significant changes in the randomness parameter in the low-force regime.

The model presented here neglects certain features such as the presence of two heads of dynein instead of only one as it is presently simplified to, three secondary sites capable of

rendering further drive or regulation through additional hydrolysis or ATP binding, and the possibility of reverse hydrolysis. The mechanochemical cycle is also oversimplified in our model. Despite these, we believe that predictions from our analysis can be tested through carefully designed experiments as they would provide an indirect verification of the crucial assumptions set in the model, such as the increase in ATP binding affinity of the secondary sites with increasing load and dependence of the step size of the molecule on the number of ATP-bound secondary sites. The analytical approach gives explicit expressions of the velocity and the fluctuation in the displacement in terms of various rate constants and one can also isolate the contributions of different secondary sites. We, therefore, believe that the use of site directed mutants that specifically inhibit the ATPase activity of different AAA subdomains, together with other biochemical tools and single molecule experiments, may be required to isolate the contributions of the secondary sites. The experimental knowledge thus generated regarding the roles of different secondary sites in powering or regulating the motion of the molecule will make it possible to further modify the model suitably. The model presented here is the first phenomenological step toward understanding the complete molecular model of dynein.

[1] B. Alberts, D. Bray, and J. Lewis, *Molecular Biology of the Cell* (Garland, New York, 1994).
[2] S. A. Burgess, M. A. Walker, H. Sakakibara, P. J. Knight, and K. Oiwa, Nature (London) **421**, 715 (2003).
[3] R. Mallik, B. C. Carter, S. A. Lex, S. J. King, and S. P. Gross, Nature (London) **427**, 649 (2004).
[4] S. Toba, T. M. Watanabe, L. Y. Okimoto, Y. Y. Toyoshima, and H. Higuchi, Proc. Natl. Acad. Sci. U.S.A. **103**, 5741 (2006).
[5] M. Schnitzer and S. Block, Cold Spring Harbor Symp. Quant. Biol. **60**, 793 (1995).
[6] K. Svoboda, P. P. Mitra, and S. M. Block, Proc. Natl. Acad. Sci. U.S.A. **91**, 11782 (1994).
[7] E. Hirakawa, H. Higuchi, and Y. Y. Toyoshima, Proc. Natl. Acad. Sci. U.S.A. **97**, 2533 (2000).
[8] D. M. Goedecke and T. C. Elston, J. Theor. Biol. **232**, 27 (2005).
[9] M. P. Singh, R. Mallik, S. P. Gross, and C. Y. Clare, Proc. Natl. Acad. Sci. U.S.A. **102**, 12059 (2005).
[10] P. Xie, S. X. Dou, and P. Y. Wang, Acta Biochim. Biophys. Sin. (Shanghai) **38**, 711 (2006).
[11] R. A. Cross, Curr. Biol. **14**, R355 (2004).
[12] S. M. King, J. Cell Sci. **113**, 2521 (2000); M. Samso and M. P. Koonce, J. Mol. Biol. **340**, 1059 (2004).
[13] S. L. Reck-Peterson and R. D. Vale, Proc. Natl. Acad. Sci. U.S.A. **101**, 1491 (2004).
[14] T. Kon, M. Nishiura, R. Ohkura, Y. Y. Toyoshima, and K. Sutoh, Biochemistry **43**, 11266 (2004).
[15] Y. Takahashi, M. Edamatsu, and Y. Y. Toyoshima, Proc. Natl. Acad. Sci. U.S.A. **101**, 12865 (2004).
[16] T. Mogami, T. Kon, K. Ito, and K. Sutoh, J. Biol. Chem. **282**, 21639 (2007).
[17] A. Silvanovich, M. G. Li, M. Serr, S. Mische, and T. S. Hays, Mol. Biol. Cell **14**, 1355 (2003).
[18] T. Shima, K. Imamula, T. Kon, R. Ohkura, and K. Sutoh, J. Struct. Biol. **156**, 182 (2006).
[19] S. Leibler and D. A. Huse, J. Cell Biol. **121**, 1357 (1993).
[20] M. E. Fisher and A. B. Kolomeisky, Physica A **274**, 241 (1999); M. E. Fisher and A. B. Kolomeisky, Proc. Natl. Acad. Sci. U.S.A. **96**, 6597 (1999).
[21] A. Mogilner, A. J. Fisher, and R. J. Baskin, J. Theor. Biol. **211**, 143 (2001).
[22] T. C. Elston, J. Math. Biol. **41**, 189 (2000).